Inversion of azimuthal PP-wave amplitudes without NMO correction for fracture weaknesses

Huaizhen Chen and Kris Innanen

Shanghai
Dec 3, 2021

NSERC CRSNG
UNIVERSITY OF CALGARY
FACULTY OF SCIENCE
Department of Geoscience

Outline

- Introduction
- Theory and method
- Numerical examples
- Conclusions

Introduction

AVAZ is more obvious at large offset

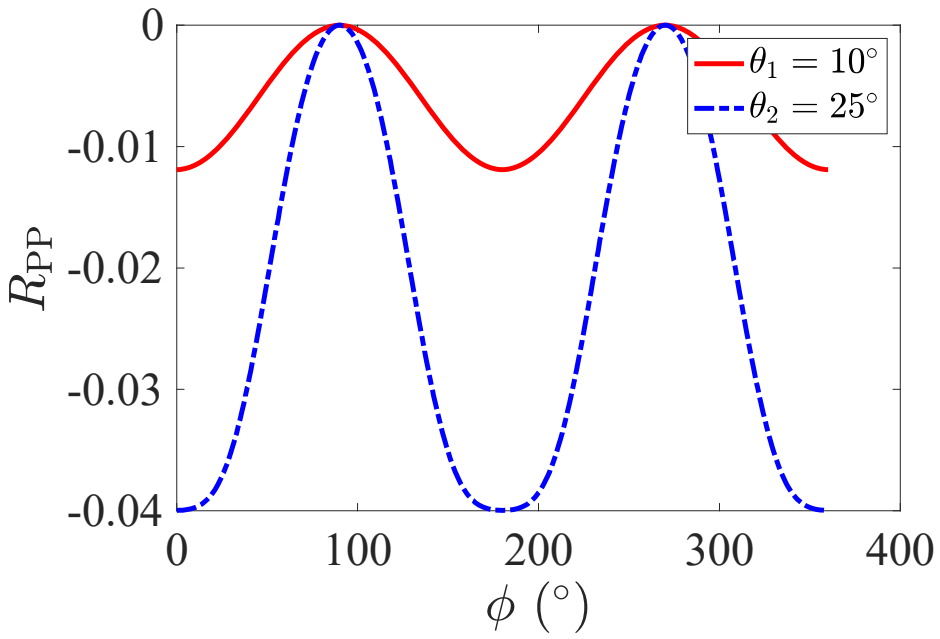

P-wave velocity variation with azimuthal angle (VVAZ)

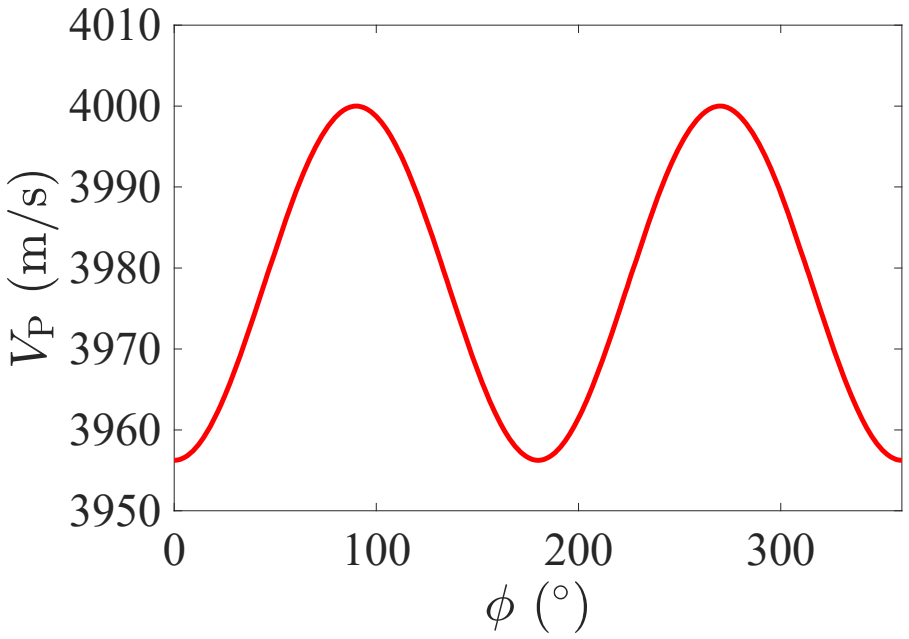

Introduction

NMO stretching and muting

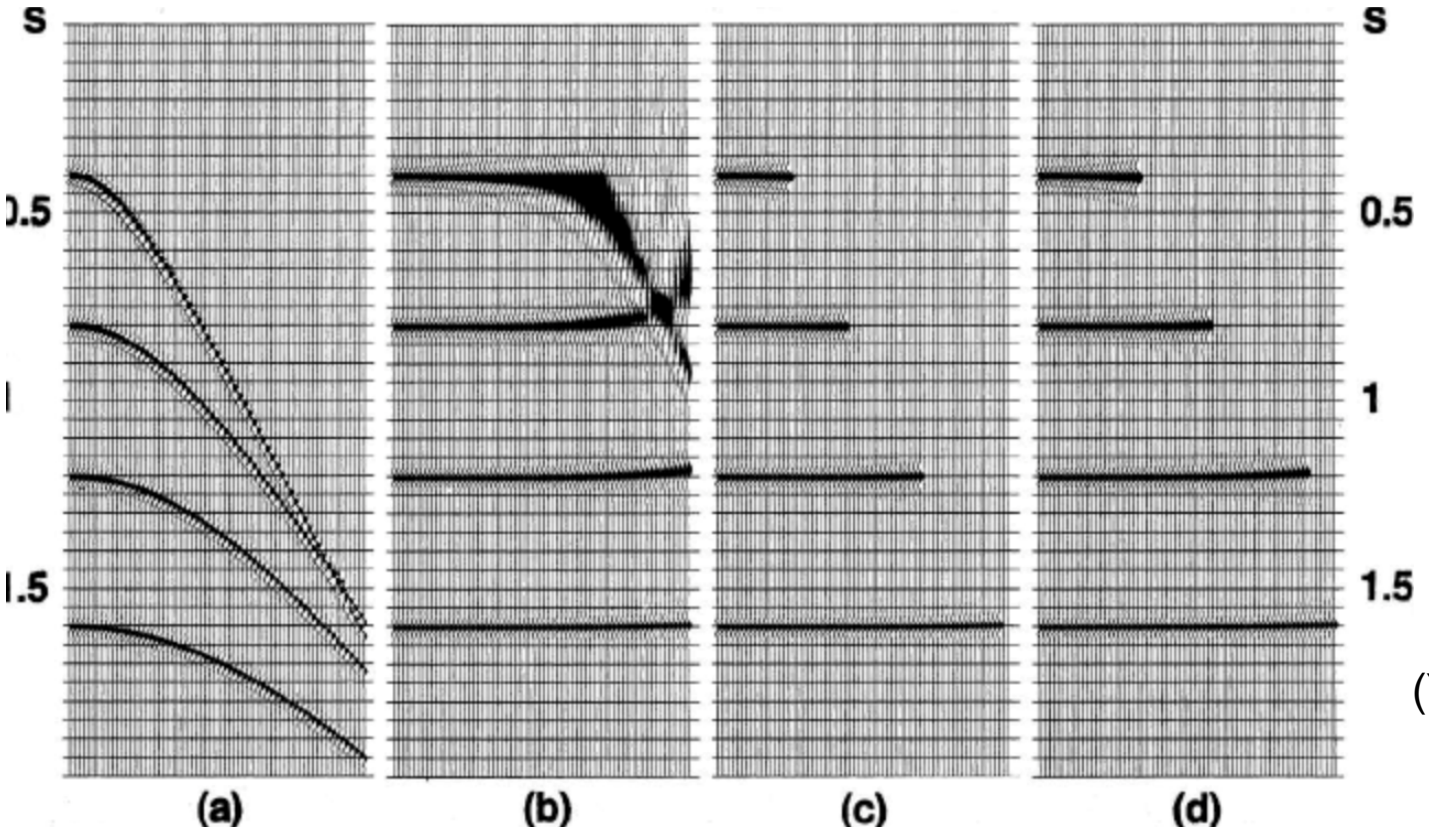

(Yilmaz, 2001)

Theory and method: Vp in HTI media

P-wave velocity expressed in terms of anisotropic parameters

$$V_{\mathrm{P}}(\theta,\phi) = \alpha\left(1+\delta\,\sin^2\theta\cos^2\theta\cos^2\phi+\varepsilon\,\sin^4\theta\cos^4\phi\right)$$

(Ruger, 1996)

P-wave velocity expressed in terms of fracture weaknesses

$$V_{\mathrm{P}}(\theta,\phi)\approx\alpha\left\{1-2g\left[(1-2g)\cos^2\theta+(1-g)\sin^2\theta\cos^2\phi\right]\sin^2\theta\cos^2\phi\,\delta_{\mathrm{N}}\right.$$
$$\left.-2g\,\sin^2\theta\cos^2\theta\cos^2\phi\,\delta_{\mathrm{T}}\right\}$$

Theory and method: Rpp in HTI media

PP-wave reflection coefficient from the solution of Zoeppritz equations

$$R_{\mathrm{PP}} = \frac{c_1 d_2 - c_3 d_4}{d_1 d_2 + d_4 d_3},$$ (Ikelle and Amundsen, 2018)

PP-wave reflection coefficient and EI in HTI media

$$\begin{aligned} R_{\mathrm{PP}}(\theta,\phi) \approx & a_{\mathrm{p}}(\theta)\, r_{\mathrm{p}} + a_{\mathrm{s}}(\theta) r_{\mathrm{s}} + a_{\mathrm{d}}(\theta) r_{\mathrm{d}} \\ & + a_{\mathrm{N}}(\theta,\phi)\Delta\delta_{\mathrm{N}} + a_{\mathrm{T}}(\theta,\phi)\Delta\delta_{\mathrm{T}} \end{aligned}$$

$$\mathrm{EI}(\theta,\phi) = \alpha^{a_{\mathrm{p}}(\theta)}\ \beta^{a_{\mathrm{s}}(\theta)}\ \rho^{a_{\mathrm{d}}(\theta)}\ \exp\left[2a_{\mathrm{N}}(\theta,\phi)\delta_{\mathrm{N}} + 2a_{\mathrm{T}}(\theta,\phi)\delta_{\mathrm{T}}\right],$$

Theory and me

Comparison between results of P-wave reflection coefficient

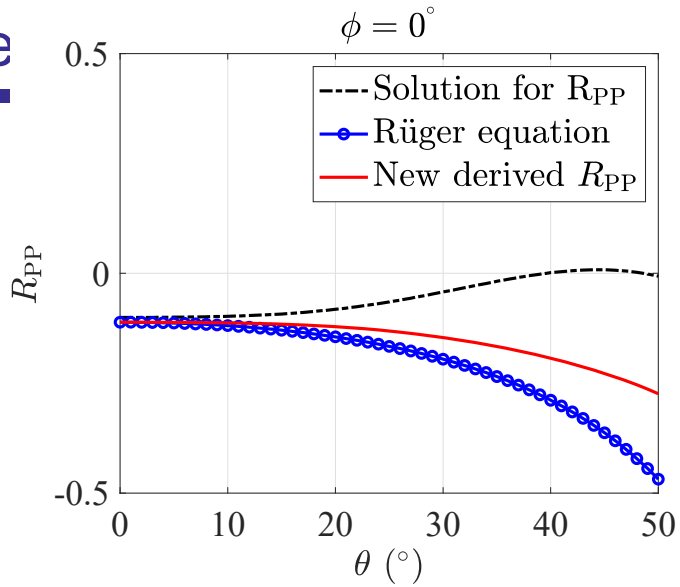

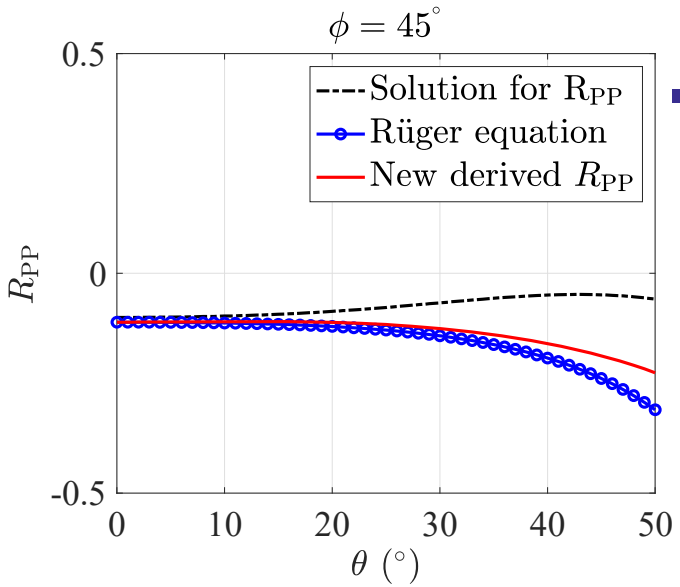

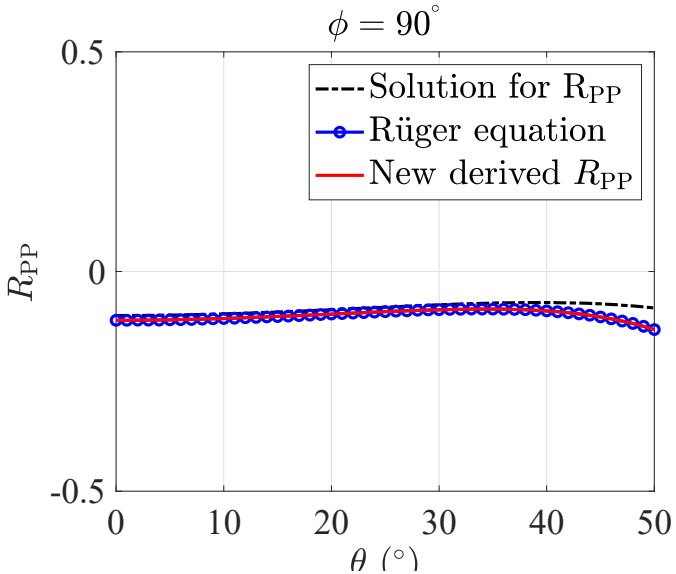

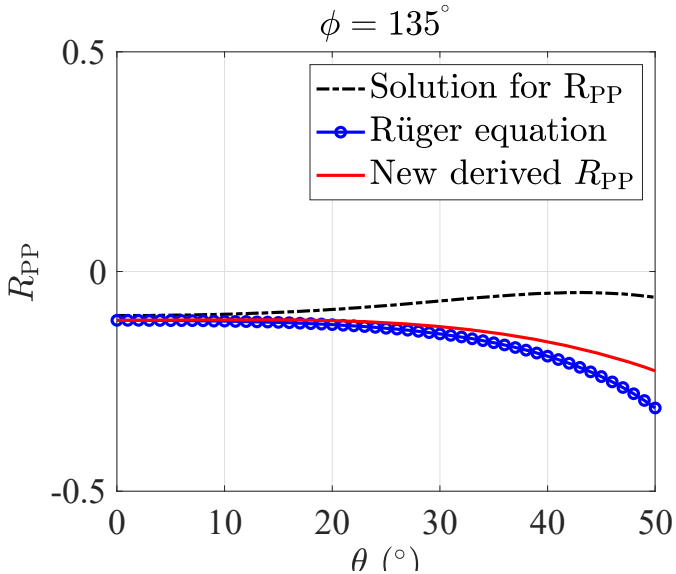

Theory and method: Bayesian Inversion for EI

The convolution model with NMO operator

$$\mathbf{s} = \mathbf{W}\,\mathbf{N}\,\mathbf{D}\,\mathbf{e},$$

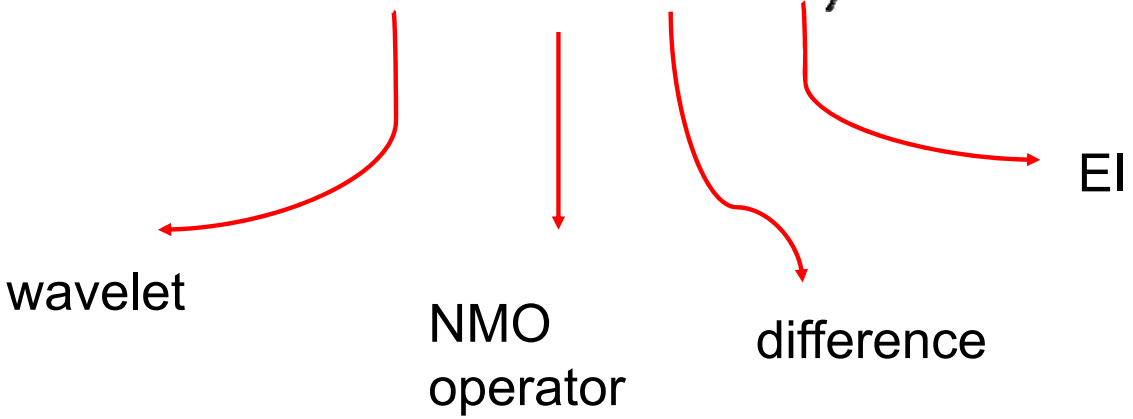

Theory and method: Bayesian Inversion for Fracture Indicators

Input data: difference in azimuthal EI

$$\mathbf{d} = \mathbf{G}\mathbf{m}$$

$$\mathbf{d} = \begin{bmatrix} \log(\mathrm{EI}(t_1, \theta_1, \phi_k)/\mathrm{EI}(t_1, \theta_1, \phi_1)) \\ \vdots \\ \log(\mathrm{EI}(t_{n+1}, \theta_1, \phi_k)/\mathrm{EI}(t_{n+1}, \theta_1, \phi_1)) \\ \\ \vdots \\ \log(\mathrm{EI}(t_1, \theta_l, \phi_k)/\mathrm{EI}(t_1, \theta_l, \phi_1)) \\ \vdots \\ \log(\mathrm{EI}(t_{n+1}, \theta_l, \phi_k)/\mathrm{EI}(t_{n+1}, \theta_l, \phi_1)) \end{bmatrix},$$

$$\mathbf{G} = \begin{bmatrix} \mathbf{p}_{\mathrm{N}}(\theta_1, \phi_1, \phi_k) & \mathbf{p}_{\mathrm{T}}(\theta_1, \phi_1, \phi_k) \\ \vdots & \vdots \\ \mathbf{p}_{\mathrm{N}}(\theta_l, \phi_1, \phi_k) & \mathbf{p}_{\mathrm{T}}(\theta_l, \phi_1, \phi_k) \end{bmatrix}$$

$$\mathbf{m} = \begin{bmatrix} \boldsymbol{\delta}_{\mathrm{N}} \\ \\ \boldsymbol{\delta}_{\mathrm{T}} \end{bmatrix}$$

Numerical examples: synthetic

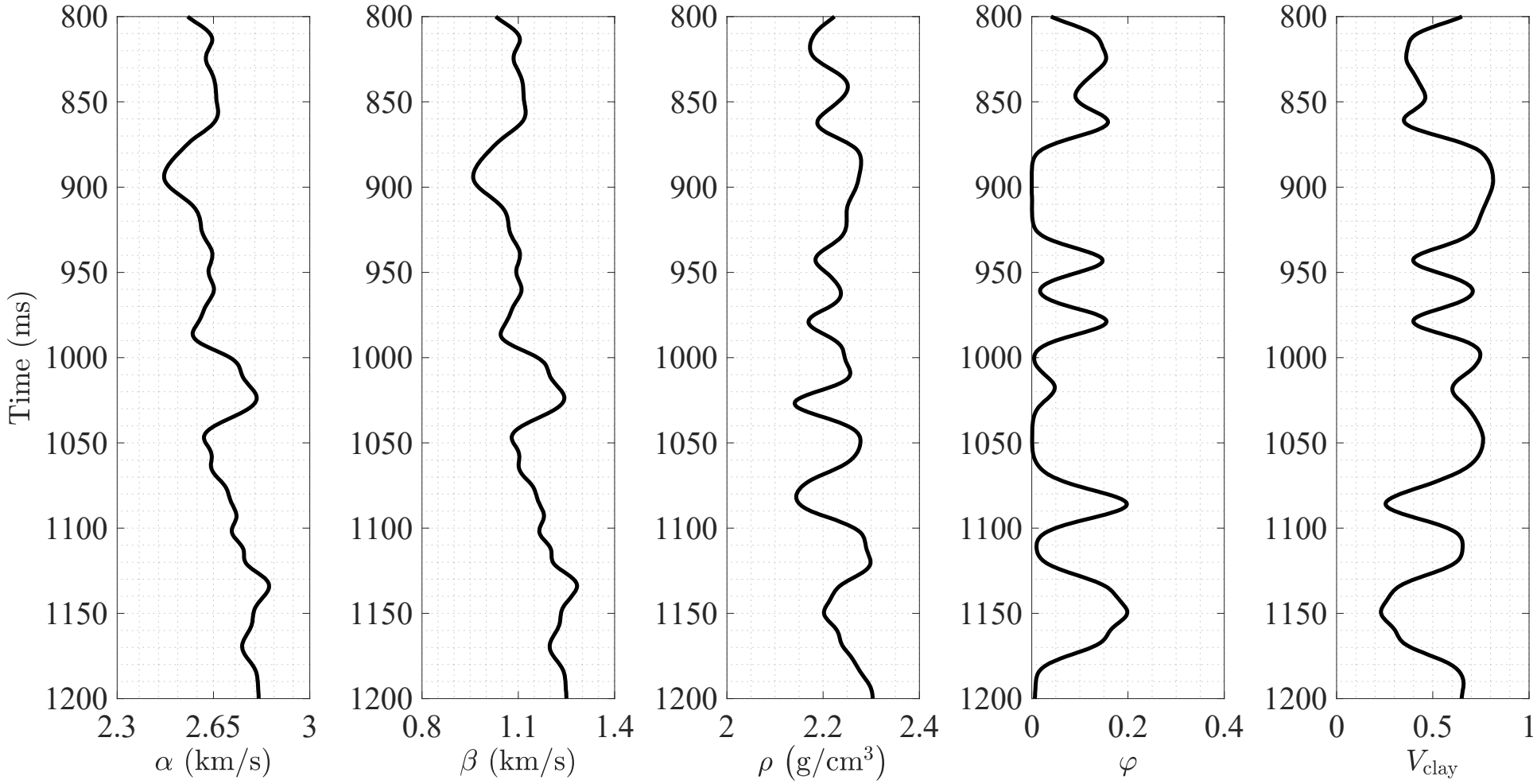

Numerical examples: synthetic

Empirical relationships between fracture weaknesses and clay volume

$$\delta_{\mathrm{N}} \approx \frac{0.6\ V_{\mathrm{clay}}\ (\alpha - 1.5)}{4.55 - 2.65\ V_{\mathrm{clay}}} \frac{1}{2g\,(1-g)},$$

$$\delta_{\mathrm{T}} \approx \frac{1.34\ V_{\mathrm{clay}}\ \beta}{4.09 - 2.29\ V_{\mathrm{clay}}}.$$

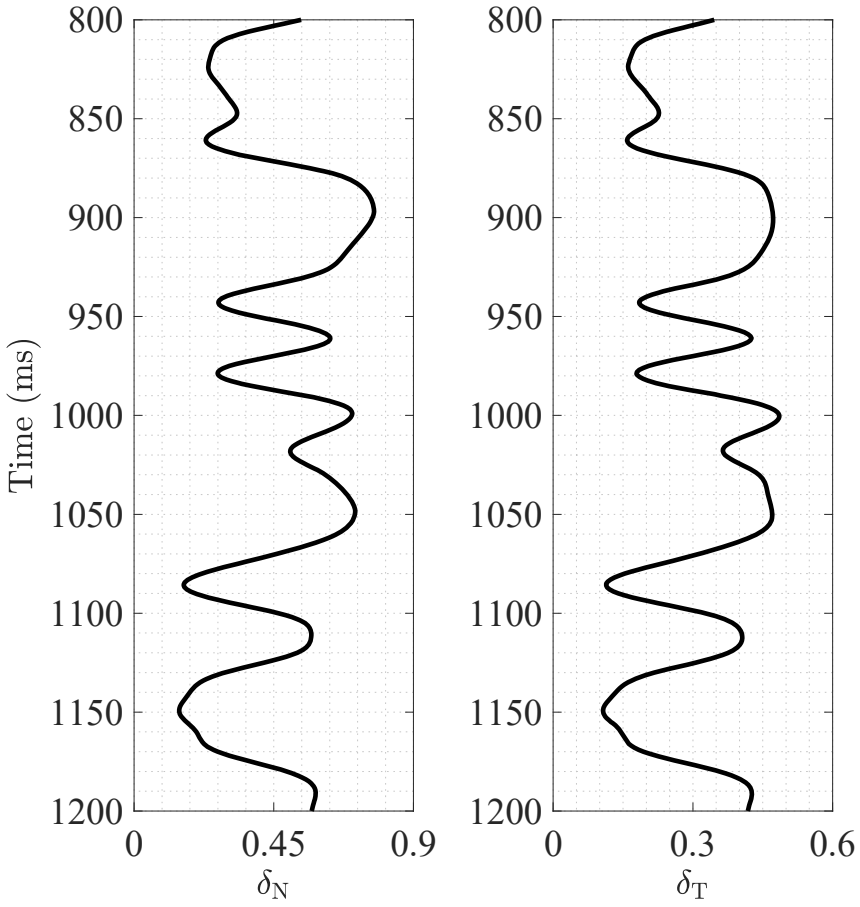

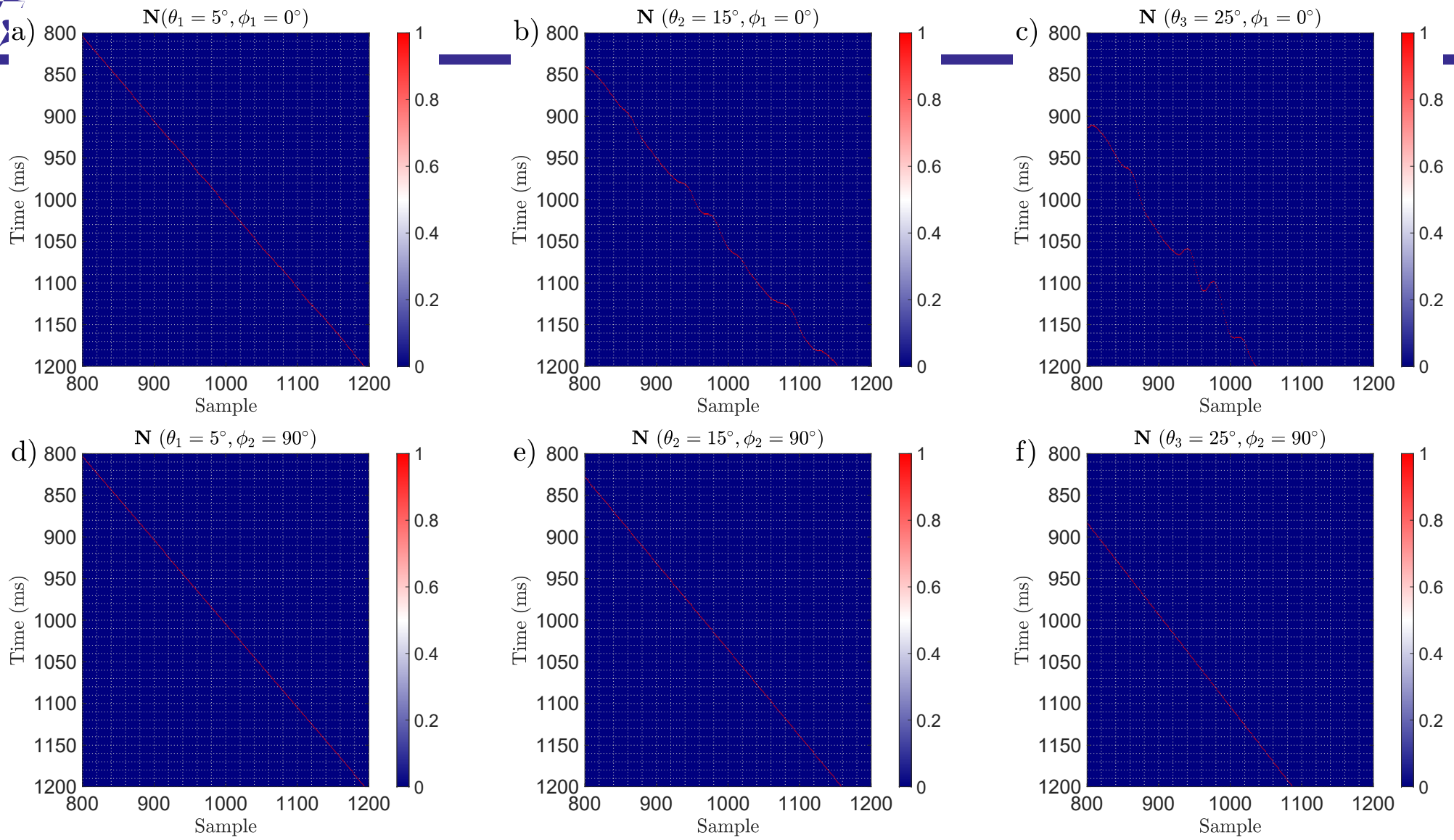
a) $\mathbf{N}(\theta_1 = 5°, \phi_1 = 0°)$
b) $\mathbf{N}\ (\theta_2 = 15°, \phi_1 = 0°)$
c) $\mathbf{N}\ (\theta_3 = 25°, \phi_1 = 0°)$
d) $\mathbf{N}\ (\theta_1 = 5°, \phi_2 = 90°)$
e) $\mathbf{N}\ (\theta_2 = 15°, \phi_2 = 90°)$
f) $\mathbf{N}\ (\theta_3 = 25°, \phi_2 = 90°)$
Time (ms)
Sample
800
850
900
950
1000
1050
1100
1150
1200
0
0.2
0.4
0.6
0.8
1

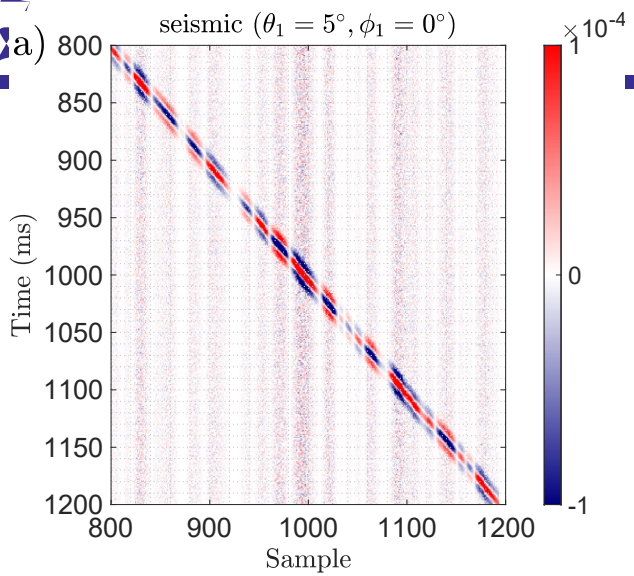
a)
seismic ($\theta_1 = 5°, \phi_1 = 0°$)
Time (ms)
Sample
$\times 10^{-4}$

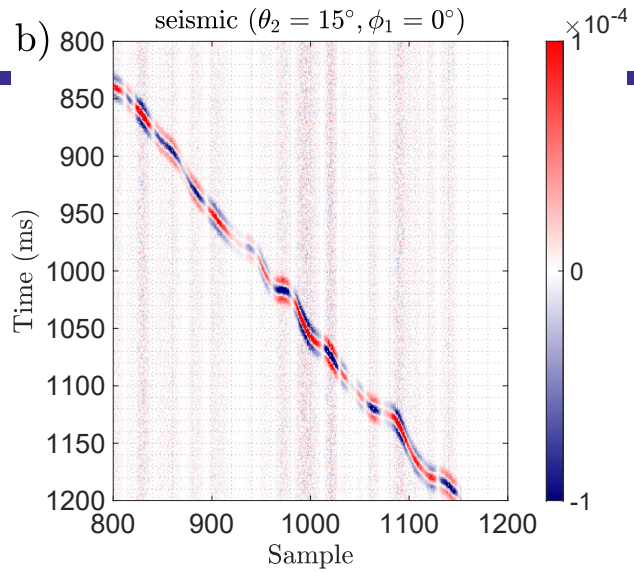
b)
seismic ($\theta_2 = 15°, \phi_1 = 0°$)
Time (ms)
Sample
$\times 10^{-4}$

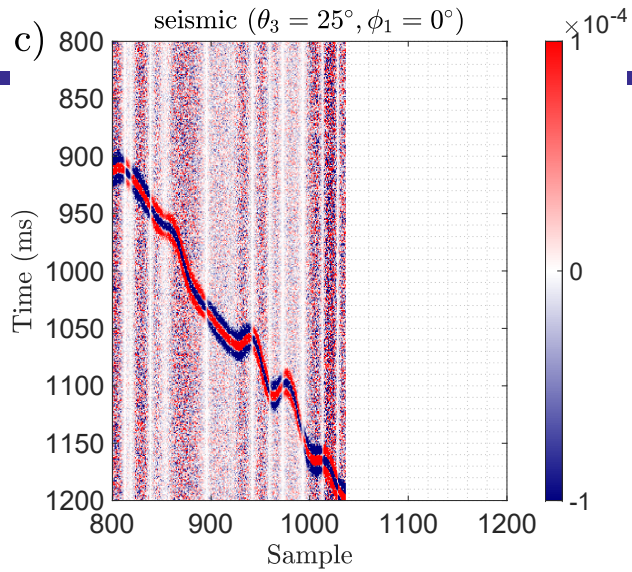
c)
seismic ($\theta_3 = 25°, \phi_1 = 0°$)
Time (ms)
Sample
$\times 10^{-4}$

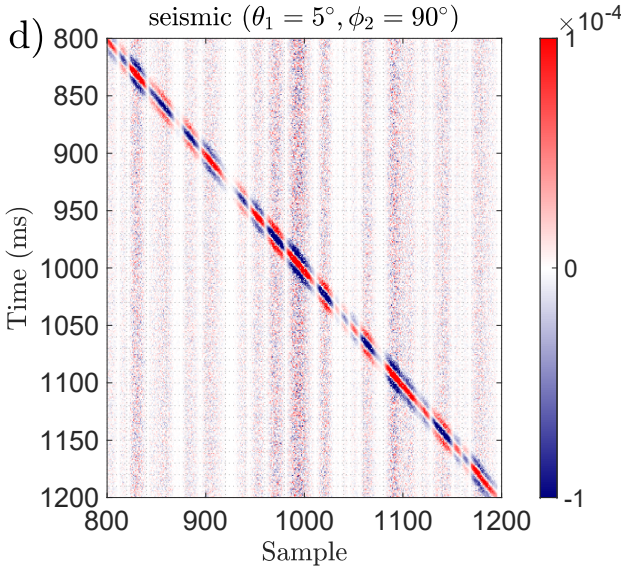
d)
seismic ($\theta_1 = 5°, \phi_2 = 90°$)
Time (ms)
Sample
$\times 10^{-4}$

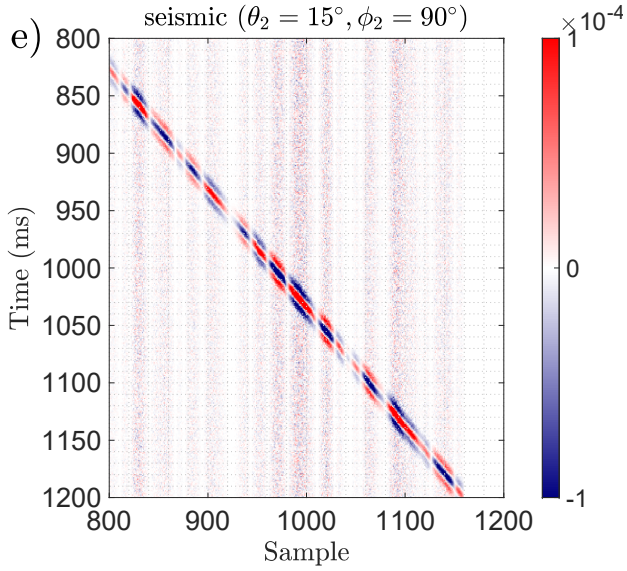
e)
seismic ($\theta_2 = 15°, \phi_2 = 90°$)
Time (ms)
Sample
$\times 10^{-4}$

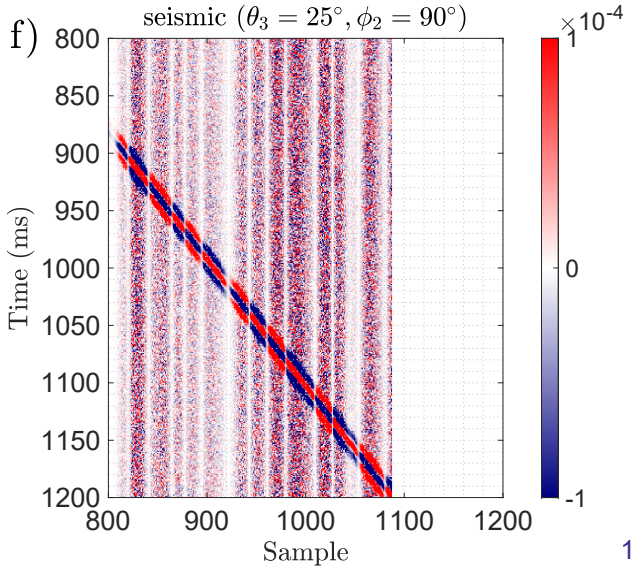
f)
seismic ($\theta_3 = 25°, \phi_2 = 90°$)
Time (ms)
Sample
$\times 10^{-4}$

Numerical examples: synthetic

Inversion for LEI

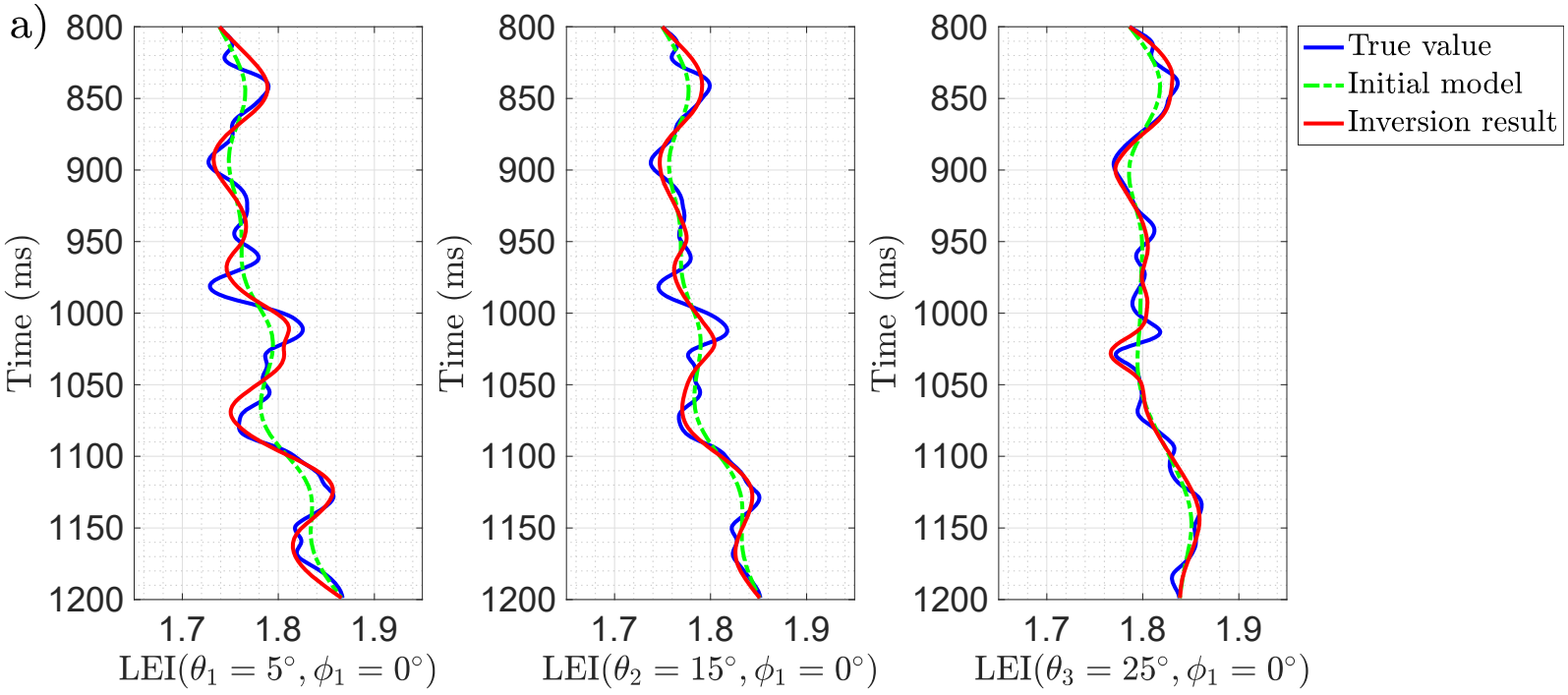

$\phi_1 = 0^\circ$

Numerical examples: synthetic

Inversion for LEI

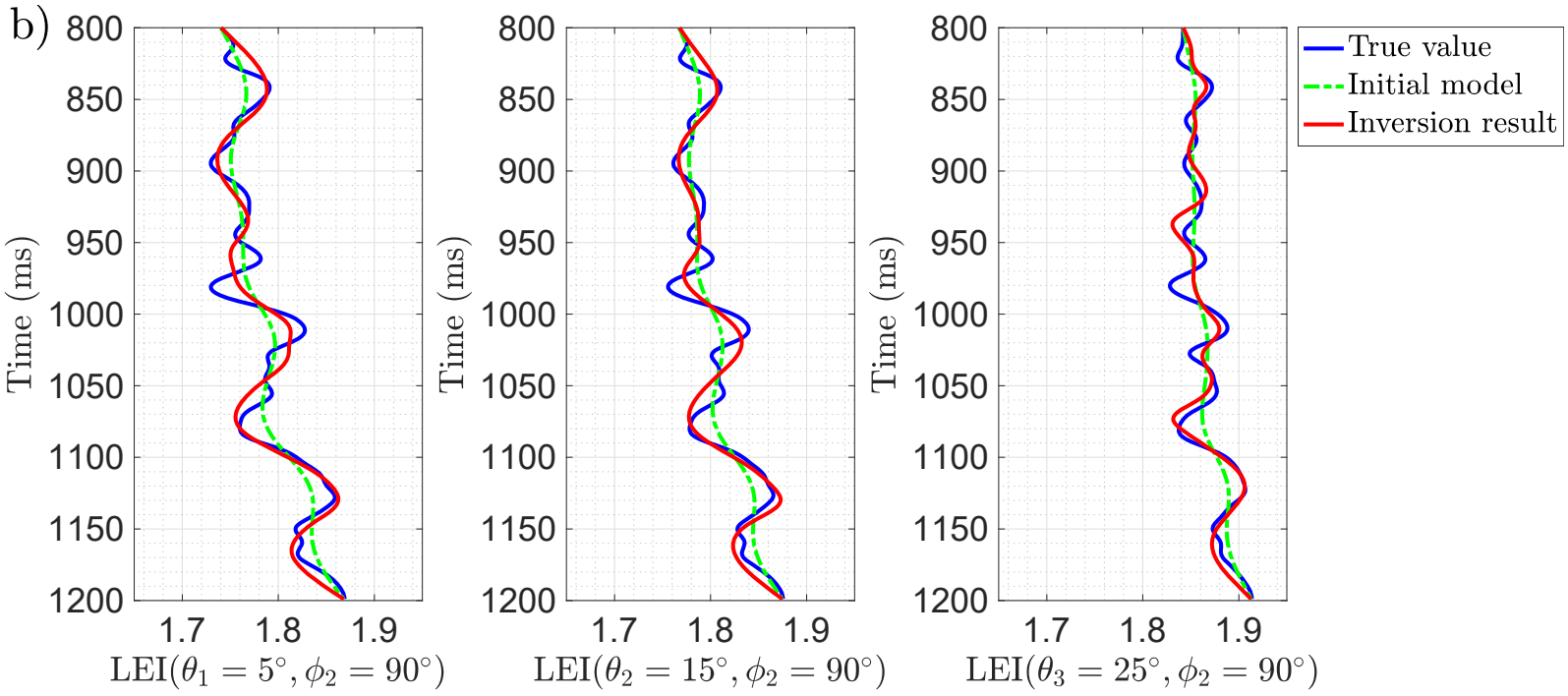

$$\phi_2 = 90°$$

Numerical examples: synthetic

Comparison between true values and inversion results of fracture weaknesses

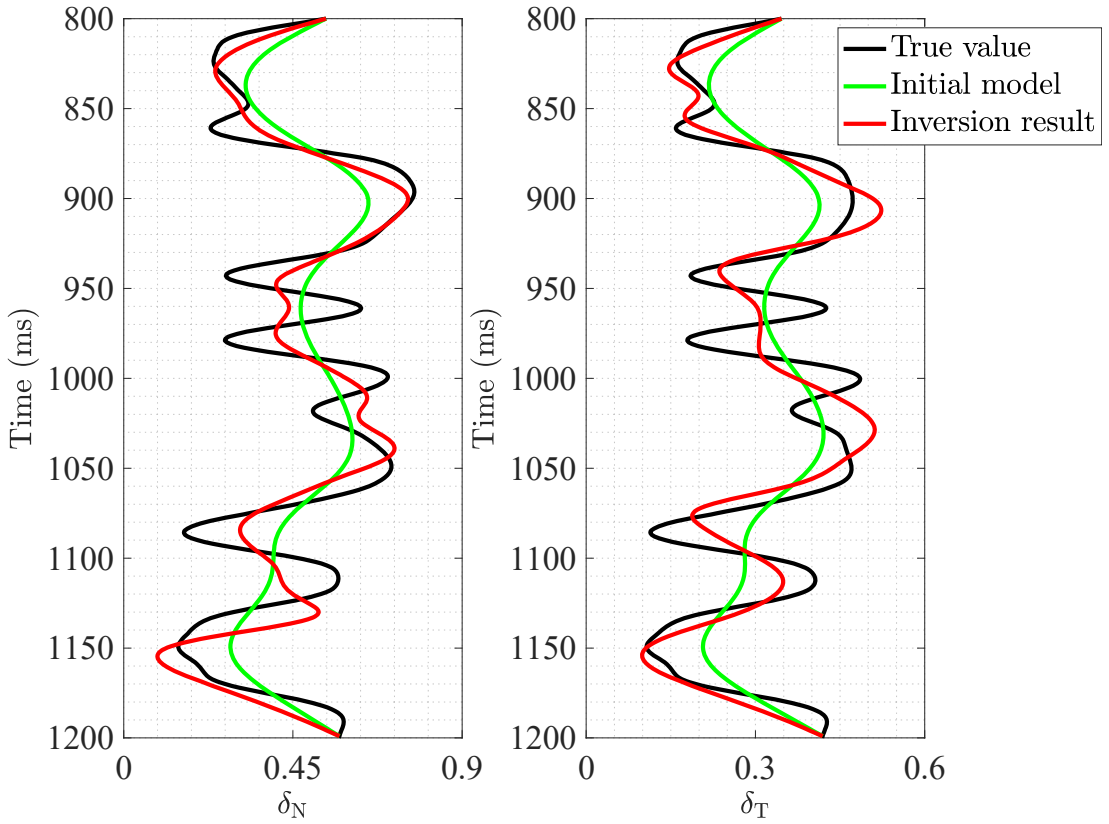

Numerical examples: Real data

Seismic gathers of different incidence and azimuthal angles (VVAZ and AVAZ)

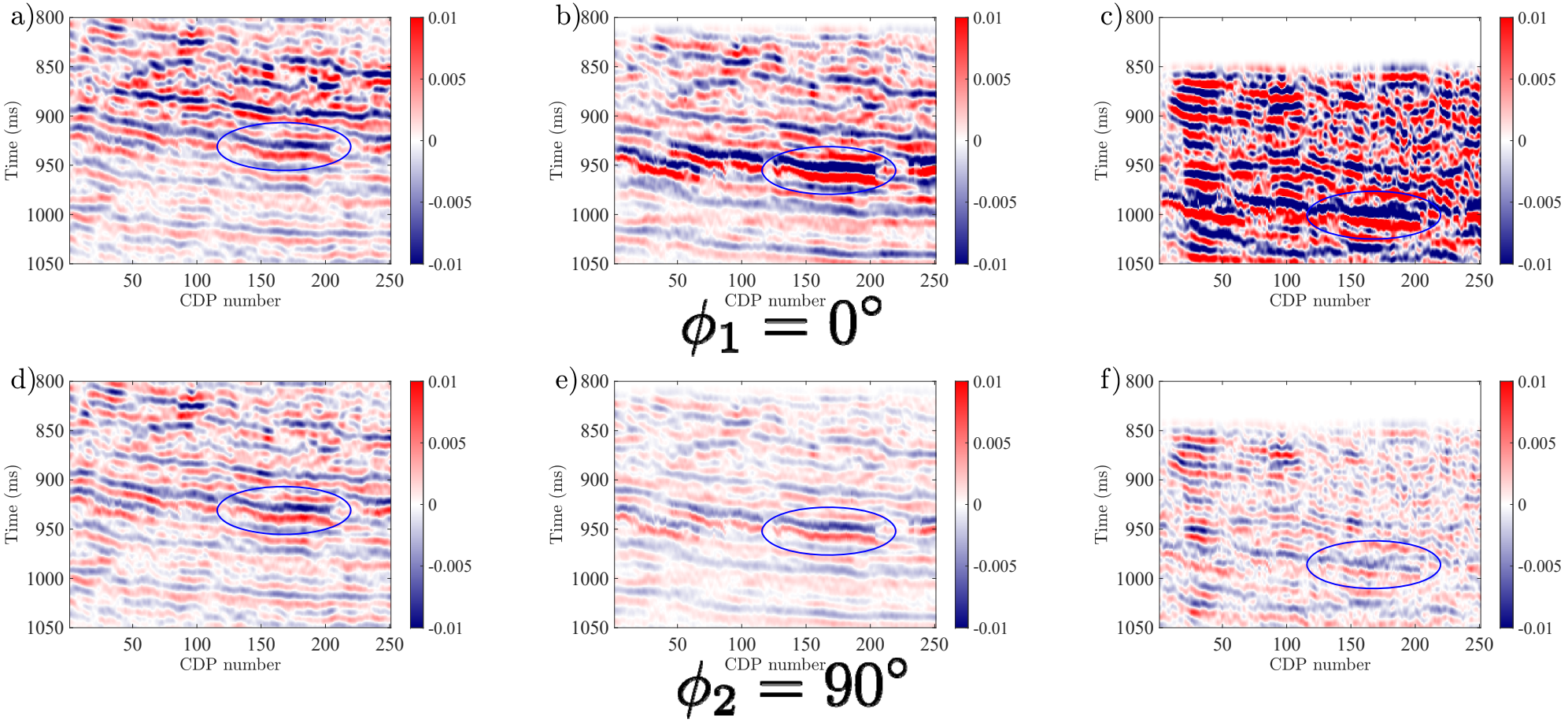

Numerical examples: Real data

Inversion results of LEI of different incidence and azimuthal angles

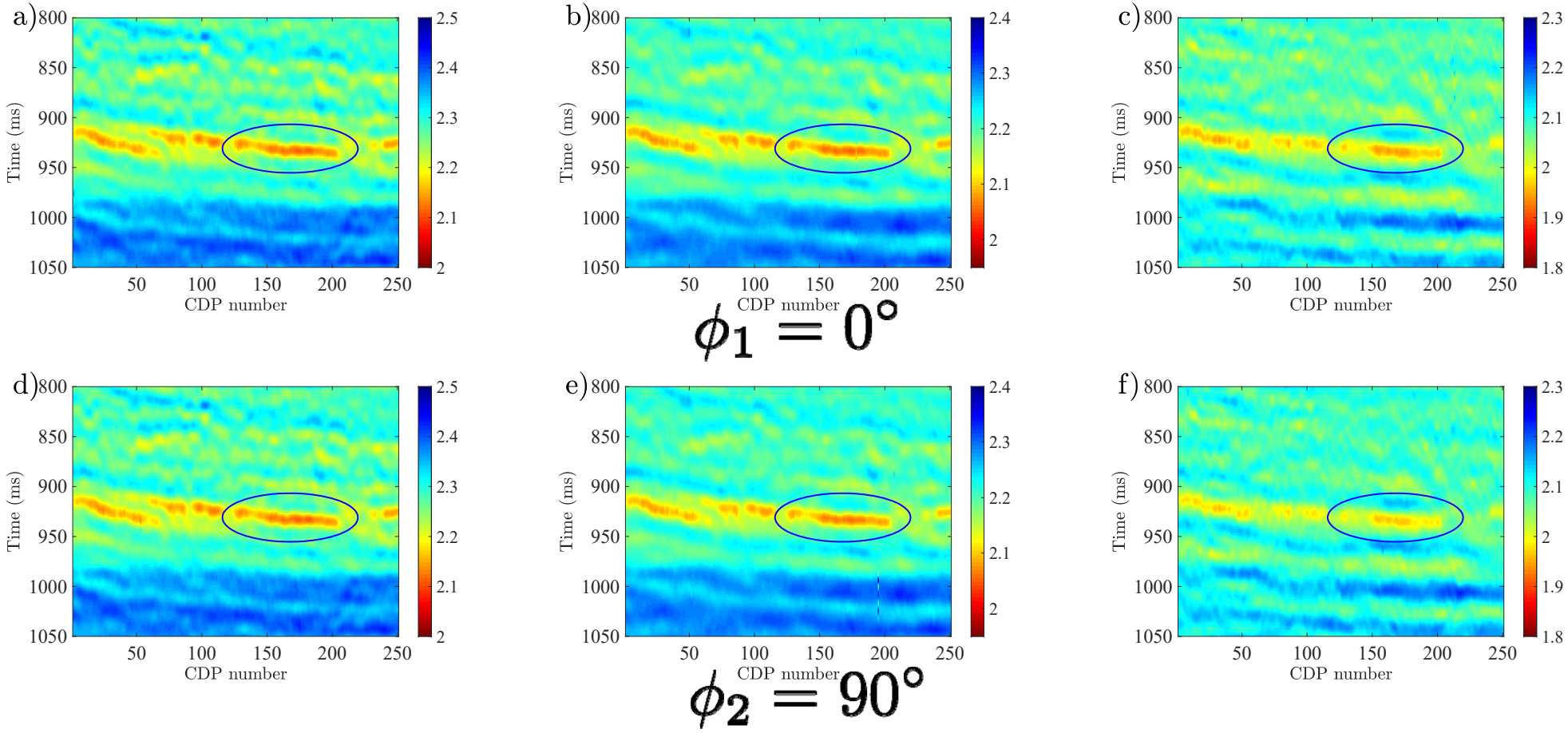

Numerical examples: Real data

Inversion results of fracture weaknesses

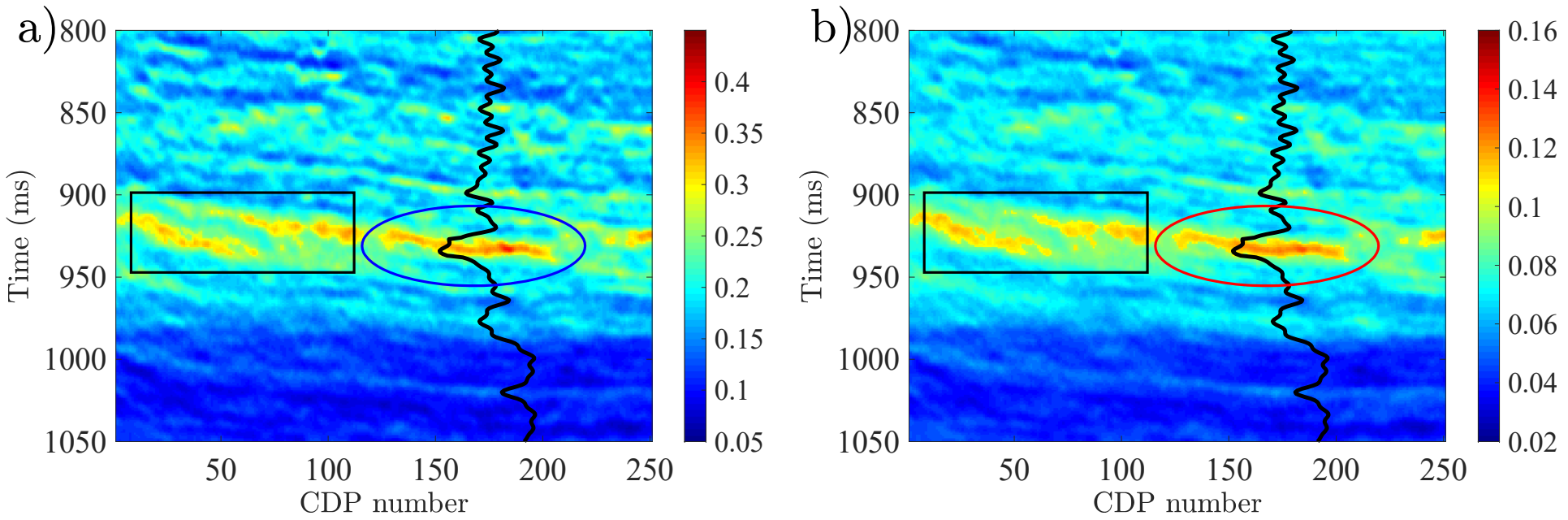

Conclusions

- We introduce a NMO operator to re-express the convolution model to generate seismic gathers without NMO correction based on the new derived Rpp and EI;

- We propose an inversion approach and workflow of employing azimuthal seismic gathers without NMO correction to estimate fracture weaknesses, which combines features of VVAZ and AVAZ;

- Tests on synthetic and real datasets confirm the robustness of the proposed inversion approach, and reliable fracture weaknesses can be obtained for the identification of potential fractured reservoirs.

Acknowledgments

- CREWES sponsors
- Tongji University
- Shanghai Sailing project and the Fundamental Research Funds for the Central Universities
- CREWES faculty, staff and students

Thank you